ELSEVIER

Remote Sensing of Environment 84 (2003) 385–392

Remote Sensing of Environment

www.elsevier.com/locate/rse

Sensitivity of vegetation indices to atmospheric aerosols: continental-scale observations in Northern Asia

Xiangming Xiao*, Bobby Braswell, Qingyuan Zhang, Stephen Boles, Stephen Frolking, Berrien Moore III

Complex Systems Research Center, Institute for the Study of Earth, Oceans and Space, University of New Hampshire, Durham, NH 03824, USA

Received 4 June 2002; received in revised form 13 August 2002; accepted 24 August 2002

Abstract

Satellite observations play an important role in characterization of the interannual variation of vegetation. Here, we report anomalies of two vegetation indices for Northern Asia (40°N–75°N, and 45°E–179°E), using images from the SPOT-4 VEGETATION (VGT) sensor over the period of April 1, 1998 to November 20, 2001. The Normalized Difference Vegetation Index (NDVI) and Enhanced Vegetation Index (EVI), which are correlated to a number of vegetation properties (e.g., net primary production, leaf area index), were compared. The results show that there is a large disagreement between NDVI and EVI anomalies in 1998 and 1999 for Northern Asia. The NDVI anomaly in 1998 was largely affected by atmospheric contamination, predominantly aerosols from extensive forest fires in that year. The EVI anomaly in 1998 was less sensitive to residual atmospheric contamination, as it is designed to be, and thus EVI is a useful alternative vegetation index for the large-scale study of vegetation. The EVI anomaly also suggests that potential vegetation productivity in Northern Asia was highest in 1998 but declined substantially in 2001, consistent with precipitation data from 1998–2001.

Keywords: SPOT-4 VEGETATION sensor; Vegetation indices; Northern Asia; Anomaly analysis

1. Introduction

Over the past few decades, a number of vegetation indices have been developed and used for monitoring of vegetation structure and function (Bannari, Morin, Bonn, & Huete, 1995). Among these, the Normalized Difference Vegetation Index (NDVI), which uses spectral information in red and near infrared bands, is the most widely used. Case studies of NDVI as a remote sensing proxy for various characteristics of terrestrial vegetation include net primary production (Tucker & Sellers, 1986; Ruimy, Saugier, & Dedieu, 1994), growing season length (Myneni et al., 1997; Zhou et al., 2001), fire (Illera, Fernandez, & Delgado, 1996; Paltridge & Barber, 1988), land use and land cover change (Loveland et al., 2000), and biogeochemical modeling (Potter et al., 1993). However, it is known that NDVI has several limitations, including sensitivity to atmospheric conditions (Holben, 1986), saturation of NDVI values (Lillesaeter, 1982) and sensitivity to soil background (Huete, 1987). Depending on the platform, changing solar zenith angle can also be a factor (Gutman, 1999). To account for residual atmospheric contamination (e.g., aerosols) and variable soil background reflectance, the Enhanced Vegetation Index (EVI, see Data and Methods for the equation) was proposed, which directly adjusts the reflectance in the red spectral band as a function of the reflectance in the blue band (Huete, Liu, Batchily, & van Leeuwen, 1997; Liu & Huete, 1995). Although the comparison between NDVI and EVI at the scale of Landsat images illustrates the sensitivity of NDVI to atmospheric conditions, there is a need to assess these vegetation indices at continental to global scales, particularly using multi-year satellite image data. The questions this study addresses are (1) to what degree does the residual atmospheric contamination and soil background affect the spatial–temporal patterns of NDVI at large spatial scales, and (2) to what degree do other vegetation indices (e.g., EVI) that consider

* Corresponding author. Tel.: +1-603-862-3818; fax: +1-603-862-0188.

E-mail address: xiangming.xiao@unh.edu (X. Xiao).

0034-4257/02/$ - see front matter © 2002 Elsevier Science Inc. All rights reserved.
PII: S0034-4257(02)00129-3

information from additional spectral bands improve observation and monitoring of vegetation at the continental to the global scales? The objective of this study is to better understand the uncertainty of NDVI-based analyses and the potential of EVI-based analyses.

We used image data from the VEGETATION (VGT) sensor onboard the SPOT-4 satellite, which was originally designed for studying vegetation and the land surface and has a number of improvements relative to the Advanced Very High Resolution Radiometer (AVHRR) sensors onboard the National Oceanic and Atmospheric Administration (NOAA) meteorological satellites. The improvements of VGT include the use of two additional spectral bands (blue and short-wave infrared). The blue band is primarily used for atmospheric correction, and the short-wave infrared (SWIR) band is sensitive to vegetation water content (Ceccato, Flasse, Tarantola, Jacquemoud, & Gregoire, 2001; Gao, 1996; Jürgens, 1997; Tucker, 1980). Multi-year global VGT data (1-km spatial resolution, daily coverage of the globe) are available for the period beginning in April 1998, and offer an unprecedented opportunity for addressing the above two scientific questions and quantifying interannual variation of vegetation indices at continental to global scales.

We have assembled 10-day composites of VGT data from April 1–10, 1998 to November 11–20, 2001 (a total of 131 observations at 10-day intervals) for Northern Asia (40°N–75°N, and 45°E–179°E). Large interannual variations in precipitation and temperature in Northern Asia can be seen over the same period (Fig. 1). As a consequence of the El Niño Southern Oscillation (ENSO) event of 1997–1998, annual precipitation was high in 1998, but declined from 1999 to 2001 (Fig. 1a). The summer of 1998 was a severe fire season in Northern Asia, and extensive fire events took place in the far east of Russia (Dlugokencky, Walter, Masarie, Lang, & Kasischke, 2001), Eastern Mongolia and Northeastern China. Biomass burning released large amounts of aerosols into the atmosphere, according to the data derived from the Total Ozone Monitoring Satellite (TOMS) (Fig. 2). These circumstances provide a unique natural experiment for us to assess the impacts of atmospheric condition and climate on vegetation indices, which would help better quantify the potential and uncertainty of vegetation indices for characterization of the interannual variation of vegetation in response to climate variability.

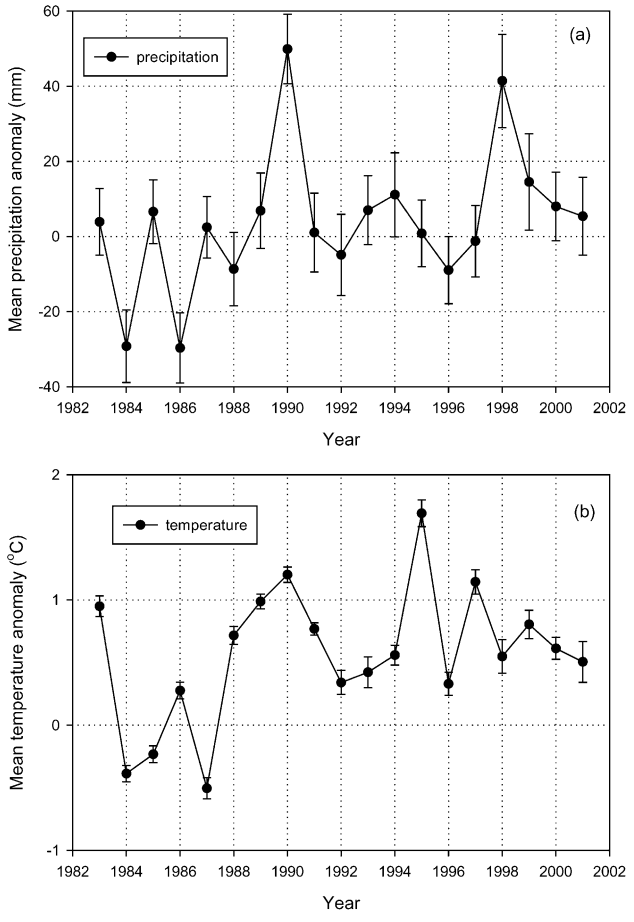

Fig. 1. Interannual variation of (a) annual precipitation and (b) temperature in Northern Asia over the period of 1/1983 to 10/2001. Precipitation and temperature data were taken from the National Climate Data Center (NCDC) Global Historical Climate Network (GHCN, http://lwf.ncdc.noaa.gov/oa/climate/research/ghcn/ghcngrid.html). The GHCN/NCDC produces anomalies of temperature and precipitation at 5° (latitude and longitude) spatial resolution based upon statistical aggregation of site data within each grid. Both precipitation anomaly and temperature anomaly were calculated with respect to the period of 1961–1990, using the traditional anomaly methods.

2. Data and methods

2.1. Multi-temporal SPOT-4 VGT sensor data

Three standard VGT products are available to users: VGT-P (Physical product), VGT-S1 (daily synthesis product) and VGT-S10 (10-day synthesis product). The spectral bands in the VGT-S1 products are estimates of ground surface reflectance, as atmospheric corrections for ozone, aerosols and water vapor have been applied to the VGT-P images using the simplified method for atmospheric correction algorithm (SMAC) described by Rahman and Dedieu (1994). The physical data used as input to SMAC are water vapor data from Meteo-France, a climatology of ozone, a simple static model for aerosols, and a 8/112° resolution Digital Elevation Model for atmospheric pressure estimation (Passot, 2000). To minimize the effects of cloud cover and variability in atmospheric optical depth, VGT-S10 data are generated by the selection of VGT-S1 pixels that have the maximum NDVI values within a 10-day period. In this study, we acquired VGT-S10 data from April 1, 1998 to November 20, 2001 (a time series of 131 observations) to cover Northern Asia (http://www.free.vgt.vito.be).

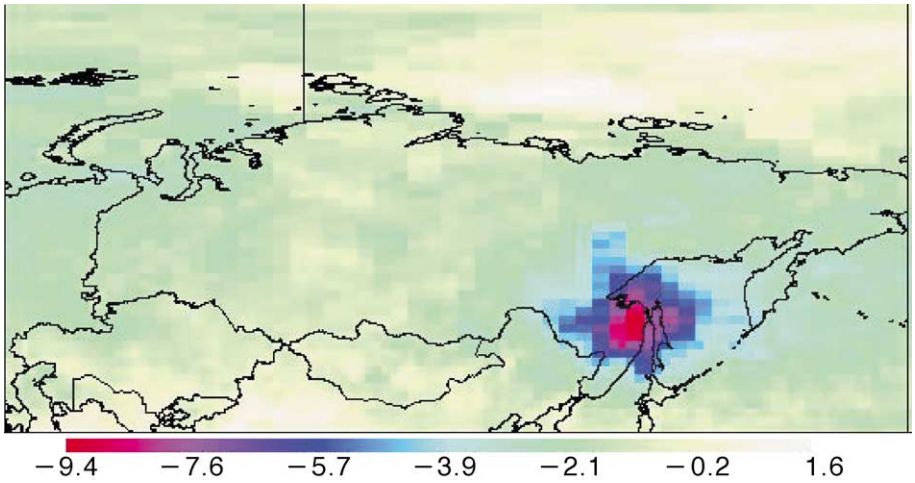

Fig. 2. The spatial distribution of the differences of tropospheric aerosols in Northern Asia between 1998 and 1999. The negative values represent a higher amount of tropospheric aerosols in 1998 than 1999. The tropospheric aerosol index data were derived from the Total Ozone Monitoring Satellite (TOMS), which are available to the public from the website of NASA Goddard Institute for Space Studies (http://www.giss.nasa.gov/data/si2000/trop.aer/).

2.2. Vegetation indices and correction of cloudy pixels

Two spectral vegetation indices were calculated for all the 10-day observations from April 1–10, 1998 to November 11–20, 2001: Normalized Difference Vegetation Index (NDVI, Rouse, Haas, Schell, Deering, & Harlan, 1974; Tucker, 1979), and Enhanced Vegetation Index (EVI, Huete et al., 1997; Justice et al., 1998; Liu & Huete, 1995):

$$\mathrm{NDVI} = \frac{\mathrm{NIR} - \mathrm{RED}}{\mathrm{NIR} + \mathrm{RED}} \tag{1}$$

$$\mathrm{EVI} = 2.5 \times \frac{\mathrm{NIR} - \mathrm{RED}}{\mathrm{NIR} + 6 \times \mathrm{RED} - 7.5 \times \mathrm{BLUE} + 1} \tag{2}$$

where the surface reflectance values of individual bands (blue, red, and NIR) are used.

The original VGT-S10 products provide a cloud quality flag in their status map files, and we designed a simple approach to fill vegetation index values for where cloudy pixels exist in the time series. Let $X(i,j,k,y)$ be the vegetation index value for pixel (i,j), composite k (varying from 1 to 36 periods in a year) and year y (varying from 1998 to 2001). For a cloudy pixel in a 10-day composite k, $X(i,j,k,y)$, we first selected a three-point time-series filter, $X(i,j,k-1,y)$, $X(i,j,k,y)$, $X(i,j,k+1,y)$ and used values of noncloudy pixels in this window to correct cloudy pixels. If both $X(i,j,k-1,y)$ and $X(i,j,k+1,y)$ pixels were cloud-free, we calculated the average of $X(i,j,k-1,y)$ and $X(i,j,k+1,y)$ and used the average value to replace $X(i,j,k,y)$. If only one pixel (either $X(i,j,k-1,y)$ or $X(i,j,k+1,y)$) was cloud-free, we used that pixel to replace $X(i,j,k,y)$. If the algorithm did not succeed in a three-point filter, we then extended to a five-point time-series filter, $X(i,j,k-2,y)$, $X(i,j,k-1,y)$, $X(i,j,k,y)$, $X(i,j,k+1,y)$, $X(i,j,k+2,y)$, using the same procedure as the above three-point filter.

2.3. Anomaly analysis of time-series vegetation index data

Time-series data of vegetation indices contain intraannual seasonality that is often much stronger than the interannual signal we wish to examine. We removed this seasonality by defining a mean annual cycle,

$$\bar{X}(i,j,k) = \frac{1}{N_y} \sum_{y=1998}^{2001} X(i,j,k,y) \tag{3}$$

where N_y is the number of years ($N_y = 3$ or 4, dependent upon k). The anomaly (deviation to the mean) is calculated by difference as

$$\mathrm{d}(i,j,k,y) = X(i,j,k,y) - \bar{X}(i,j,k) \tag{4}$$

Spatial and temporal averages of vegetation index anomalies for Northern Asia were calculated as the average of the deviation from the mean

$$\bar{D}_{\mathrm{s}}(k,y) = \left[\sum_{i=1,j=1}^{m,n} \mathrm{d}(i,j,k,y) \times a(i,j) \right] \Big/ \sum_{i=1,j=1}^{m,n} a(i,j) \tag{5}$$

for all land pixels over Northern Asia for a 10-day composite k, with $m \times n$ pixels, weighted by pixel area, $a(i,j)$, noting that the area of a pixel in VGT images (geographical projection) varies with latitude. We then aggregated $\bar{D}_{\mathrm{s}}(k,y)$ by month, season (winter, spring, summer and fall) and plant growing season (April to September), respectively.

For exploring spatial variations of vegetation index (VI) anomalies, we first calculated the sum of VI anomalies at a 10-day interval over the period of April–September for individual pixels (Eq. (6)). Then, we calculated the differences of annual anomalies of vegetation indices (EVI, NDVI) between 1999 and 1998 (Eq. (7)), resulting in

thematic maps that show the spatial distribution of the changes of VI anomalies between 1999 and 1998.

$$\mathrm{VI}_y(i,j,y) = \sum_{k=\mathrm{April}}^{k=\mathrm{September}} \mathrm{d}(i,j,k,y) \quad (6)$$

$$\mathrm{VI}_{1999-1998}(i,j) = \mathrm{VI}_{1999}(i,j,1999) - \mathrm{VI}_{1998}(i,j,1998) \quad (7)$$

where y is the year (1998, 1999), and VI is NDVI or EVI, respectively. We constructed a two-way contingency table that describes whether $\mathrm{NDVI}_{1999-1998}(i,j)$ and $\mathrm{EVI}_{1999-1998}(i,j)$ agree or disagree with each other, assuming three scenarios: $\mathrm{VI}_{1999-1998}(i,j)<0$, $\mathrm{VI}_{1999-1998}(i,j)=0$, $\mathrm{VI}_{1999-1998}(i,j)>0$. This results in a thematic map of agreement/disagreement between NDVI and EVI annual anomalies between 1999 and 1998.

3. Results

A false color composite image of VGT-S10 data in July 1–10, 2000 clearly illustrates the spatial distribution of major land cover types (e.g., forest, grassland, desert, tundra) in Northern Asia (Fig. 3a). In general, the large-scale spatial distribution of NDVI is similar to that of EVI, as NDVI and

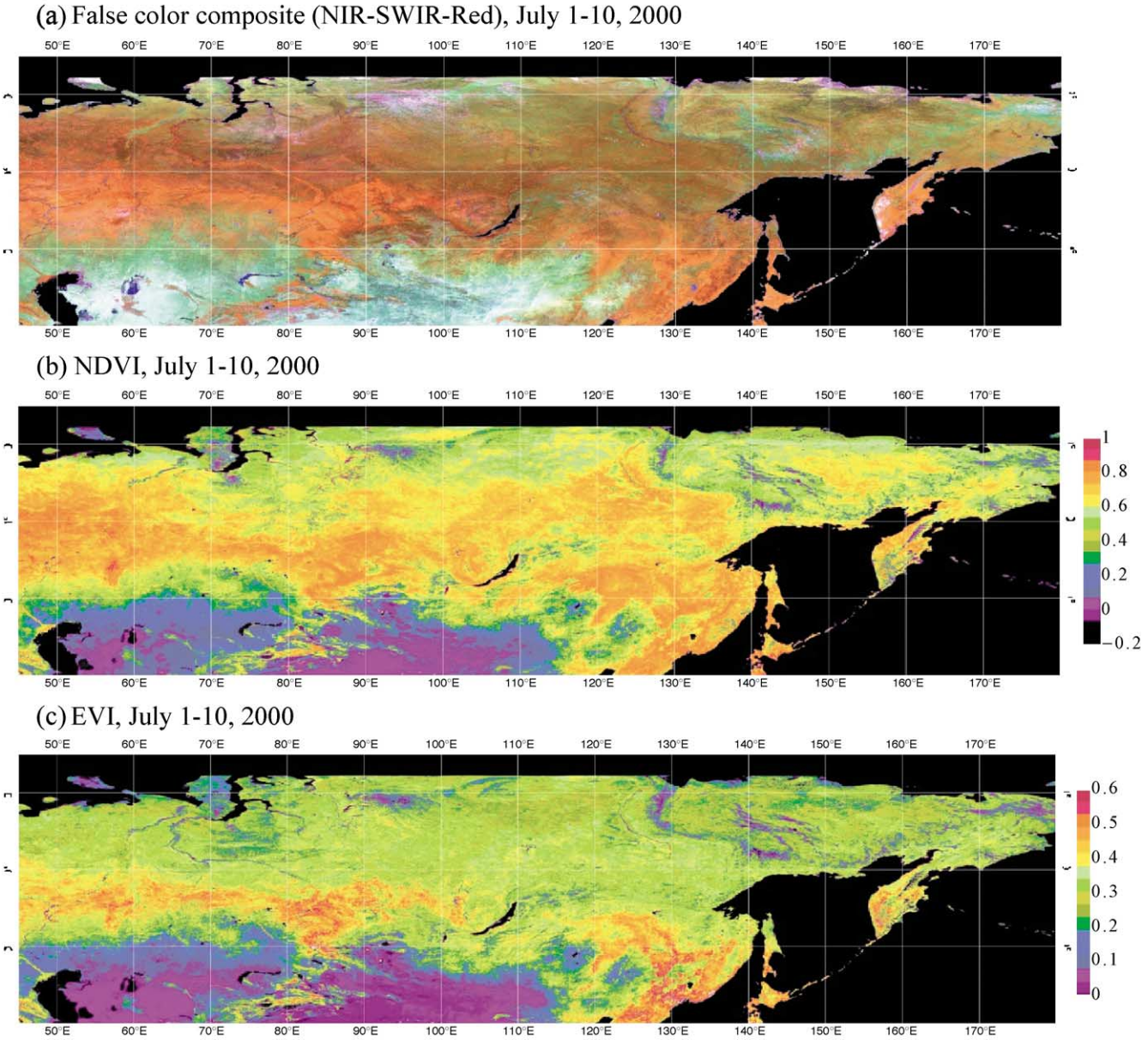

Fig. 3. The spatial distribution of vegetation characteristics in Northern Asia (40°N–75°N, 45°E–179°E), as illustrated by 10-day composite data of July 11–20, 2000 from the VEGETATION sensor onboard SPOT-4. (a) False color composite (NIR–SWIR–RED); (b) NDVI and (c) EVI.

EVI values are highest in forested regions and lowest in desert areas (Fig. 3b,c). While forests have a high and relatively uniform range of values in the NDVI image (Fig. 3b), the EVI image indicates that broadleaf forests have higher EVI values (red color in Fig. 3c) than coniferous forests, as expected due to their typically higher gap fraction.

At the continental scale, the NDVI anomaly over the plant-growing season is substantially different from the EVI anomaly for the same period (Fig. 4d). The NDVI anomaly in 1998 was well below the 4-year average and lower than in 1999. The observed NDVI anomaly in 1998 can be mostly attributed to low NDVI values in August–September (Fig. 4b). The VGT-derived NDVI anomaly was the highest in 2000 but decreased substantially in 2001 (Fig. 4d). In comparison, the EVI anomaly was much higher in 1998 than in 1999 (Fig. 4d). The EVI anomaly was at a similar level for 1999 and 2000 but decreased substantially in 2001. The precipitation anomaly was also the highest in 1998 but substantially declined in 2001 (Fig. 1a).

At the pixel level, we calculated cumulative anomalies of NDVI and EVI over the growing season (April–September) in 1998 and 1999, respectively. Differences in the cumulative NDVI anomalies between 1998 and 1999 were calculated (Fig. 5a), and the NDVI anomalies in 1999 were generally higher than in 1998. Differences of the cumulative EVI anomalies between 1998 and 1999 were also calculated (Fig. 5b), but many pixels have lower EVI anomalies in 1999 than in 1998. In order to spatially identify where NDVI and EVI anomalies differed and agreed with each other between 1999 and 1998, a thematic map was generated (Fig. 5c). The most significant disagreement between EVI and NDVI anomalies occurred in those areas that had extensive fires in 1998. Fire and biomass burning in the summer of 1998 could contribute large amounts of aerosols to the atmosphere. The tropospheric aerosol data (Torres, Bhartia, Herman, Sinyuk, & Holben, 2002), derived from the Total Ozone Monitoring Satellite (TOMS), suggest that atmospheric aerosol concentrations over the period of April to September were much higher in 1998 than in 1999 for many parts of Northern Asia (Fig. 2), corresponding well with those areas that experienced large fires in 1998. Aerosols scatter sunlight directly to the optical sensor and

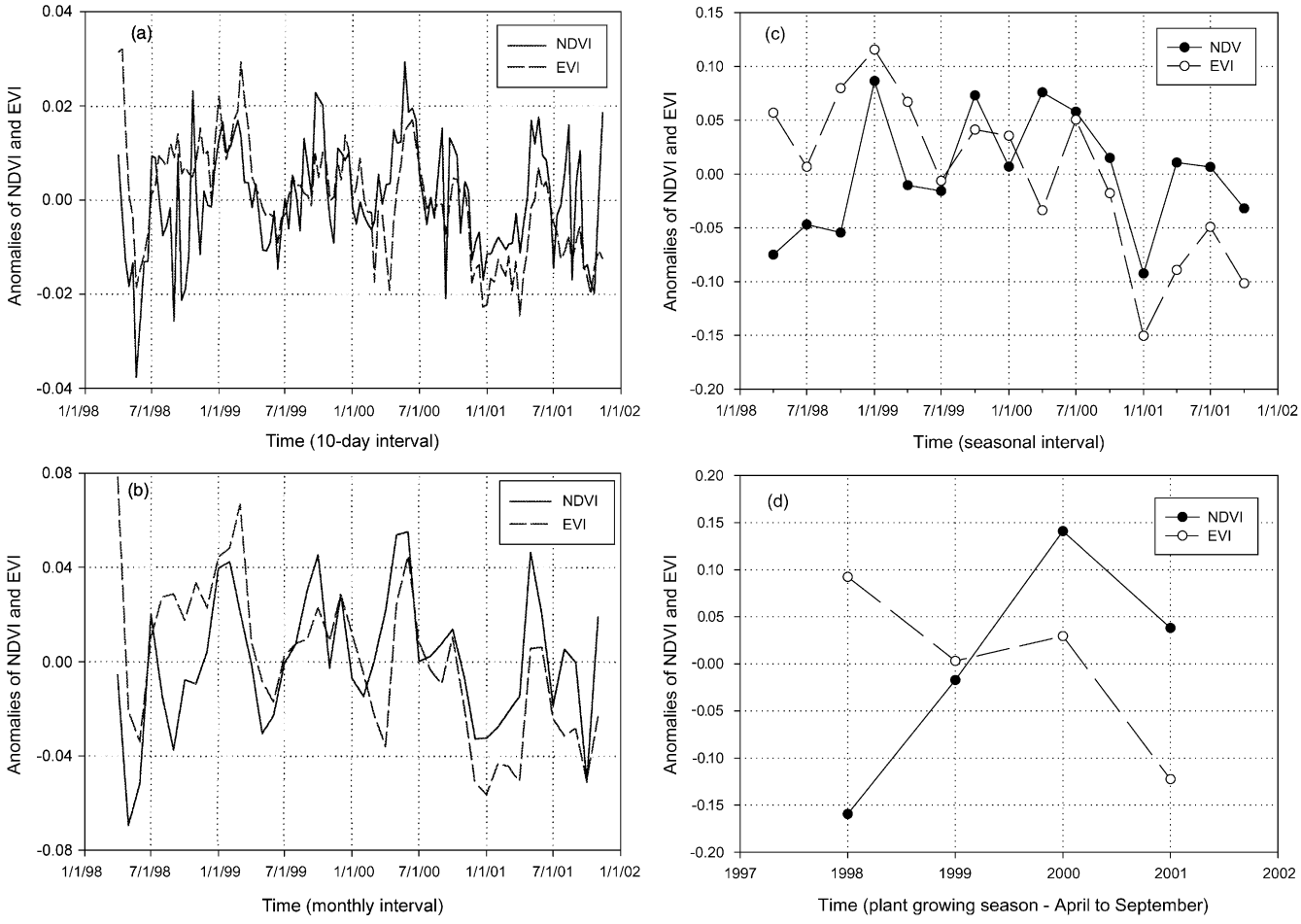

Fig. 4. Anomalies of EVI and NDVI in Northern Asia over the period of 1998 to 2001 at different temporal scales, i.e., 10-day, monthly, seasonal and plant growing season (April to September). These are the area-weighted mean NDVI and EVI anomaly values for the entire Northern Asia.

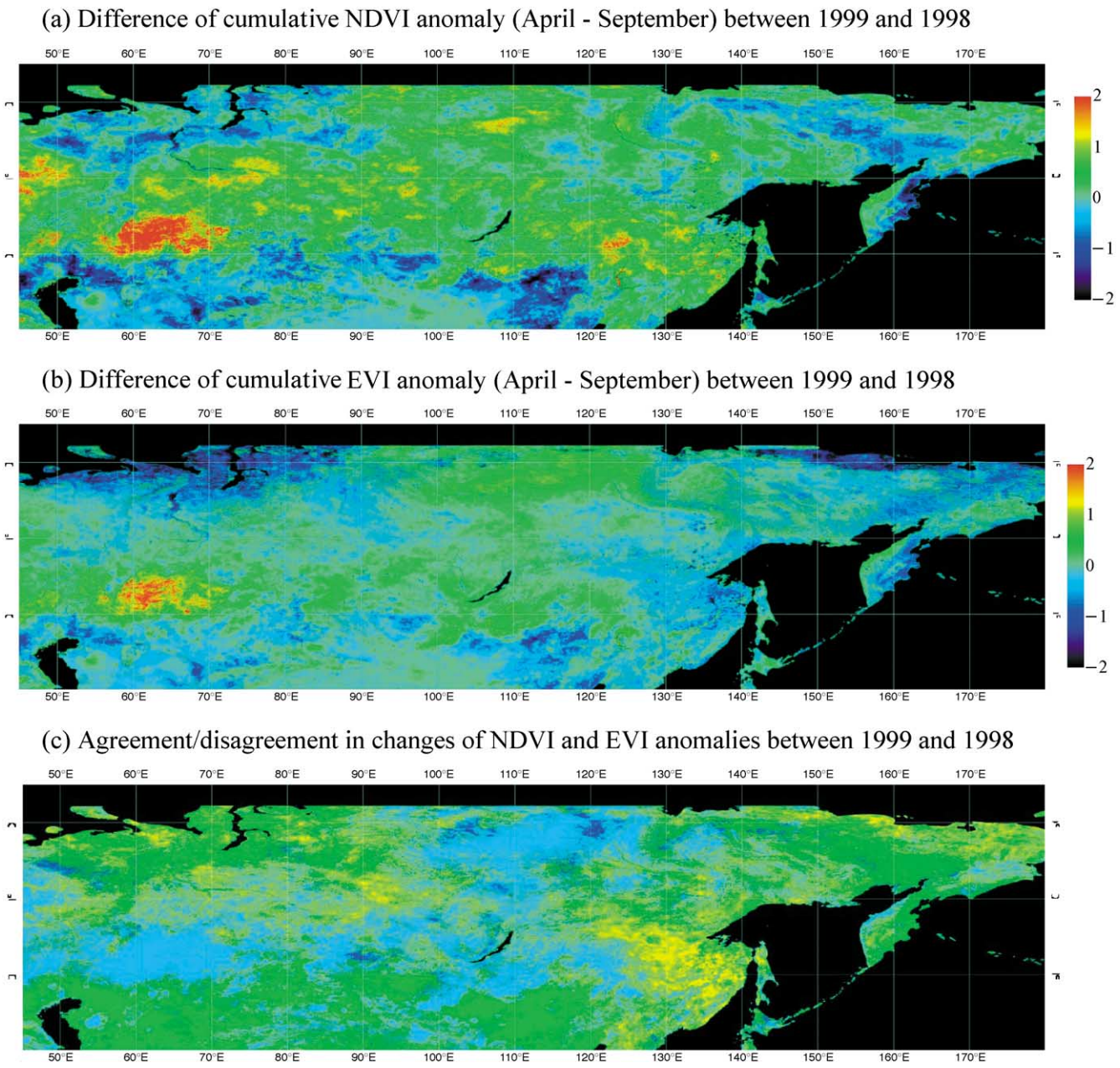

Fig. 5. The pixel-level comparison between cumulative NDVI and EVI anomalies over plant growing season (April–September) in Northern Asia. (a) The difference map of NDVI anomalies between 1998 and 1999, where positive values represent higher cumulative NDVI anomaly in 1999 than 1998; (b) the difference map of EVI anomalies between 1998 and 1999; where positive values represent higher cumulative EVI anomaly in 1999 than 1998; (c) the thematic map that describes pixel-level agreement/disagreement in annual anomalies (April to September) of EVI and NDVI in Northern Asia between 1999 and 1998. Case 1: $EVI_{1999-1998}(i,j) < 0$ and $NDVI_{1999-1998}(i,j) < 0$ (34%, green); Case 2: $EVI_{1999-1998}(i,j) > 0$ and $NDVI_{1999-1998}(i,j) < 0$ (7%, blue); Case 3: $EVI_{1999-1998}(i,j) < 0$ and $NDVI_{1999-1998}(i,j) > 0$ (23%, yellow); Case 4: $EVI_{1999-1998}(i,j) > 0$ and $NDVI_{1999-1998}(i,j) > 0$ (36%, cyan).

thus increase the apparent reflectance in red band; and aerosols also absorb sunlight and thus decrease to a lesser degree the reflectance in the near infrared band (Fraser & Kaufman, 1985; Karnieli, Kaufman, Remer, & Wald, 2001). The tropospheric aerosols apparently reduced the NDVI values in the summer of 1998, resulting in a lower NDVI anomaly in 1998 than in 1999. Because the EVI uses the blue band to account for the atmospheric aerosols, the EVI anomaly in 1998 was less affected.

4. Discussion

This continental-scale analysis of multi-year VGT data shows that there is likely a large uncertainty in the NDVI anomaly for Northern Asia, which we attribute mostly to residual atmospheric contamination (e.g., aerosols from biomass burning). In an earlier analysis of AVHRR-derived NDVI time series for the period of 1981–1999, Zhou et al. (2001) reported that the NDVI anomaly (April

to October) of Eurasia (40°N to 70°N) was lower in 1998 than in 1999, which is similar to the VGT-derived NDVI anomalies in 1998 and 1999 (Fig. 4d). The NOAA AVHRR sensors provide the longest continuous observations of the Earth, and time series of AVHRR-derived NDVI data from the early 1980s have been used and analyzed in numerous studies. Caution should be taken in interpreting time series of NDVI, especially in those years that had experienced large forest and grassland fires. Consistent with the earlier studies (Huete et al., 1997; Justice et al., 1998; Liu & Huete, 1995), this continental-scale study demonstrates that the EVI provides a useful alternative vegetation index for characterization of inter-annual variation of vegetation at large spatial scales, as it is less affected by atmospheric conditions and soil/vegetation background.

This study also shows that there were large spatial and temporal (seasonal to interannual) variations in EVI across Northern Asia over the period of 1998 to 2001. Interannual variation of vegetation in response to climate is an important issue in the global carbon cycle. The terrestrial biosphere was apparently largely neutral with respect to net carbon exchange during the 1980s, but became a much stronger net carbon sink in the 1990s (Bousquet et al., 2000; Ciais, Tans, Trolier, White, & Francey, 1995; Schimel et al., 2001). It is thought that the unusually large carbon sink in the early 1990s can be largely attributed to climate variability (Schimel et al., 2001). Eurasia and North America are the two most likely regions that account for the large and controversial net carbon sink of the terrestrial biosphere in the 1990s (Fang, Cheng, Peng, Zhao, & Ci, 2000; Rayner, Enting, Francey, & Langenfelds, 1999; Schimel et al., 2001). This sink has been linked to vegetation response to environmental change, and has been shown to exhibit strong interannual fluctuations. Increases in the growth of temperate and boreal forests in response to longer growing seasons may have contributed significantly to the carbon sink in Eurasia (Myneni et al., 2001). While EVI provides useful information about changes in vegetation over time, in order to develop quantitative relationships between the remote sensing proxies (e.g., EVI) and vegetation properties (e.g., net primary productivity, leaf area index), extensive in situ field data collection, modeling, and scaling studies are needed across various terrestrial ecosystems. There are a number of field sites that might have abundant field data for interpretation of remote sensing images, including eddy flux tower sites, the Long-Term Ecological Network in USA and the Chinese Ecosystem Research Network in China. Development of new remote sensing products (e.g., EVI-based estimates of vegetation net primary production and leaf area index, land cover classification) would provide crucial datasets for biogeochemical, hydrological and climate models in a coherent effort to understand patterns and mechanisms of net carbon exchange between the terrestrial biosphere and the atmosphere.

Acknowledgements

This study was supported by the NASA Land Use and Land Cover Change program, the NASA Earth Observing System (EOS) Interdisciplinary Science program, and the NASA Terrestrial Ecology program.

References

Bannari, A., Morin, D., Bonn, F., & Huete, A. R. (1995). A review of vegetation indices. *Remote Sensing Reviews*, *13*, 20–95.

Bousquet, P., Peylin, P., Ciais, P., LeQuere, C., Friedlingstein, P., & Tans, P. P. (2000). Regional changes in carbon dioxide fluxes of land and oceans since 1980. *Science*, *290*, 1342–1346.

Ceccato, P., Flasse, S., Tarantola, S., Jacquemoud, S., & Gregoire, J. M. (2001). Detecting vegetation leaf water content using reflectance in the optical domain. *Remote Sensing of Environment*, *77*, 22–33.

Ciais, P. P., Tans, P., Trolier, M., White, J. W. C., & Francey, R. J. (1995). A large northern hemisphere terrestrial CO_2 sink indicated by the 13C/12C ratio of atmospheric CO_2. *Science*, *269*, 1098–1102.

Dlugokencky, E. J., Walter, B. P., Masarie, K. A., Lang, P. M., & Kasischke, E. S. (2001). Measurements of an anomalous global methane increase during 1998. *Geophysical Research Letters*, *28*(3), 499–502.

Fang, J., Chen, A., Peng, C., Zhao, S., & Ci, L. (2000). Changes in forest biomass carbon storage in China between 1949 and 1998. *Science*, *292*, 2320–2322.

Fraser, R. S., & Kaufman, Y. J. (1985). The relative importance of scattering and absorption in remote sensing. *IEEE Transactions on Geoscience and Remote Sensing*, *23*, 625–633.

Gao, B. (1996). NDWI—A Normalized Difference Water Index for remote sensing of vegetation liquid water from space. *Remote Sensing of Environment*, *58*, 257–266.

Gutman, G. G. (1999). On the use of long-term global data of land reflectance and vegetation indices derived from the advanced very high resolution radiometer. *Journal of Geophysical Research*, *104*, 6241–6255.

Holben, B. (1986). Characteristics of maximum-value composite images from temporal AVHRR data. *International Journal of Remote Sensing*, *7*, 1417–1434.

Huete, A. R. (1987). Soil influence in remote sensed vegetation-canopy spectra. In C. Elachi (Ed.), *Introduction to the physics and techniques of remote sensing* (pp. 107–141). New York: Wiley-Interscience.

Huete, A. R., Liu, H. Q., Batchily, K., & van Leeuwen, W. (1997). A comparison of vegetation indices over a global set of TM images for EOS-MODIS. *Remote Sensing of Environment*, *59*, 440–451.

Illera, P., Fernandez, A., & Delgado, J. A. (1996). Temporal evolution of the NDVI as an indicator of forest fire danger. *International Journal of Remote Sensing*, *17*(6), 1093–1105.

Jürgens, C. (1997). The modified normalized difference vegetation index (mNDVI)–a new index to determine frost damages in agriculture based on Landsat TM data. *International Journal of Remote Sensing*, *18*, 3583–3594.

Justice, C. O., Vermote, E., Townshend, J. R. G., Defries, R., Roy, D. P., Hall, D. K., Salomonson, V. V., Privette, J. L., Riggs, G., Strahler, A., Lucht, W., Myneni, R. B., Knyazikhin, Y., Running, S. W., Nemani, R. R., Wan, Z., Huete, A. R., van Leeuwen, W., Wolfe, R. E., Giglio, L., Muller, J. P., Lewis, P., & Barnsley, M. J. (1998). The Moderate Resolution Imaging Spectroradiometer (MODIS): land remote sensing for global change research. *IEEE Transactions on Geoscience and Remote Sensing*, *36*(4), 1228–1249.

Karnieli, A., Kaufman, Y. J., Remer, L., & Wald, A. (2001). AFRI—aerosol free vegetation index. *Remote Sensing of Environment*, *77*, 10–21.

Lillesaeter, O. (1982). Spectral reflectance of partly transmitting leaves: laboratory measurements and mathematical modeling. *Remote Sensing of Environment*, *12*, 247–254.

Liu, H. Q., & Huete, A. R. (1995). A feedback based modification of the NDVI to minimize canopy background and atmospheric noise. *IEEE Transactions on Geoscience and Remote Sensing*, *33*, 457–465.

Loveland, T. R., Reed, B. C., Brown, J. F., Ohlen, D. O., Zhu, Z., Yang, L., & Merchant, J. W. (2000). Development of a global land cover characteristics database and IGBP DIScover from 1-km AVHRR data. *International Journal of Remote Sensing*, *6*(7), 1303–1330.

Myneni, R. B., Dong, J., Tucker, C. J., Kaufmann, R. K., Kauppi, P. E., Zhou, L., Alexeyev, V., & Hughes, M. K. (2001). A large carbon sink in the woody biomass of Northern forests. *Proceedings of the National Academy of Sciences*, *98*(26), 14784–14789.

Myneni, R. B., Keeling, C. D., Tucker, C. J., Asrar, G., & Nemani, R. R. (1997). Increased plant growth in the northern high latitudes from 1981–1991. *Nature*, *386*, 698–702.

Paltridge, G. W., & Barber, J. (1988). Monitoring grassland dryness and fire potential in Australia with NOAA-AVHRR data. *Remote Sensing of Environment*, *25*, 381–394.

Passot, X. (2000). VEGETATION image processing methods in the CTIV. In Saint G. (Ed.), *Proceedings of VEGETATION 2000: 2 years of operation to prepare the future*. International Conference of VEGETATION 2000, April 3–6, 2000, Lake Maggiore, Italy.

Potter, C. S., Randerson, J. T., Field, C. B., Matson, P. A., Vitousek, P. M., Mooney, H. A., & Klooster, S. A. (1993). Terrestrial ecosystem production: a process model based on global satellite and surface data. *Global Biogeochemical Cycles*, *7*(4), 811–841.

Rahman, H., & Dedieu, G. (1994). SMAC: a simplified method for atmospheric correction of satellite measurements in the solar spectrum. *International Journal of Remote Sensing*, *15*, 123–143.

Rayner, P. J., Enting, I. G., Francey, R. J., & Langenfelds, R. (1999). Reconstructing the recent carbon cycle from atmospheric CO_2, $\delta^{13}C$, and O_2/N_2 observations. *Tellus*, *B51*, 213–232.

Rouse, J. W., Haas, R. H., Schell, J. A., Deering, D. W., & Harlan, J. C. (1974). Monitoring the vernal advancements and retrogradation (greenwave effect) of nature vegetation (371 pp.). NASA/GSFC Final Report, Greenbelt, MD.

Ruimy, A., Saugier, B., & Dedieu, G. (1994). Methodology for the estimation of terrestrial net primary production from remotely sensed data. *Journal of Geophysical Research*, *99*(D3), 5263–5283.

Schimel, D., House, J. I., Hibbard, K. A., Bousquest, P., Ciais, P., Peylin, P., Braswell, B. H., Apps, M. J., Baker, D., Bondeau, A., Canadell, J., Churkina, G., Cramer, W., Denning, A. S., Field, C., Friedlingstein, P., Goodale, C., Heimann, M., Houghton, R. A., Melillo, J. M., Moore III, B., Murdiyarso, D., Nobles, I., Pacala, S. W., Prentice, I. C., Raupach, M. R., Rayner, P. J., Scholes, R. J., Steffen, W. J., & Wirth, C. (2001). Recent patterns and mechanisms of carbon exchange by terrestrial ecosystems. *Nature*, *414*, 169–172.

Torres, O., Bhartia, P. K., Herman, J. R., Sinyuk, A., & Holben, B. (2002). A long term record of aerosol optical thickness from TOMS observations and comparison to AERONET measurements. *Journal of Atmospheric Science*, *59*, 398–413.

Tucker, C. J. (1979). Red and photographic infrared linear combinations for monitoring vegetation. *Remote Sensing of Environment*, *8*, 127–150.

Tucker, C. J. (1980). Remote sensing of leaf water content in the near-infrared. *Remote Sensing of Environment*, *10*, 23–32.

Tucker, C. J., & Sellers, P. J. (1986). Satellite remote sensing of primary productivity. *International Journal of Remote Sensing*, *7*, 1395–1416.

Zhou, L., Tucker, C. J., Kaufmann, R. K., Slayback, D., Shabanov, N. V., & Myneni, R. B. (2001). Variations in northern vegetation activity inferred from satellite data of vegetation index during 1981 to 1999. *Journal of Geophysical Research*, *106*(D17), 20069–20083.